Nonlinear Absorption Dynamics in Tetrapyridyl Metalloporphyrins

N. M. Barbosa Neto,*,† L. De Boni,† C. R. Mendonça,† L. Misoguti,† S. L. Queiroz,‡ L. R. Dinelli,§ A. A. Batista,§ and S. C. Zilio†

Instituto de Física de São Carlos, Universidade de São Paulo, Caixa Postal 369, 13560-970 São Carlos, SP, Brazil, Instituto de Química de São Carlos, Universidade de São Paulo, Caixa Postal 780, 13560-970 São Carlos, SP, Brazil, and Departamento de Química, Universidade Federal de São Carlos, BR-13565-905 São Carlos, SP, Brazil

Received: April 26, 2005; In Final Form: July 6, 2005

Nonlinear absorption dynamics of Zn^{2+}, Cu^{2+}, and Ni^{2+} tetrapyridyl porphyrins in chloroform/methanol solutions were investigated at 532 nm with the Z-scan technique. Additional techniques such as UV−vis absorption spectroscopy and time-resolved fluorescence were used to obtain parameters that are important for the analysis of the population dynamics. A marked difference was observed in the nonlinear absorption and excited-state dynamics of closed (ZnTPyP)- and open-shell metalloporphyrins (CuTPyP and NiTPyP). ZnTPyP presents a reverse saturable absorption whose dynamics can be completely described by means of a simple five-energy-level diagram. On the other hand, CuTPyP and NiTPyP have a different excited-state dynamics, presenting a saturable absorption behavior and faster relaxation rates that were attributed to the presence of unfilled *d* shells of the central ion.

Introduction

Porphyrins have received a great deal of attention during the past few years because they present interesting photophysical properties that place them as potential candidates for applications in optical devices such as limiters and switches.[1−3] Moreover, they are present in a wide variety of natural biological processes[4] and are used as photosensitizers in photodynamic therapy (PDT) for cancer treatment.[5] This application justifies, by itself, the ever-increasing interest in investigating this class of materials. The PDT is based on the energy transfer from excited states of the photosensitizer to molecular oxygen, and its efficacy depends on the absorption cross-sections, lifetimes, and quantum yields of these excited states. The feasibility of porphyrin-based optical devices also depends on such photophysical parameters, and thus it is clearly important to determine the absorption dynamics and excited-state characteristics of these important complexes.

Regarding the structural aspect, porphyrins are molecules where four pyrrole rings, forming a square, are connected by unsaturated methine bridges to complete a macrocycle.[6] In general, metalloporphyrins have the central part of the ring occupied by a metal ion linked to two pyrrole rings to yield the necessary structural stability. In particular, tetrapyridyl porphyrins (TPyP) have four pyridyl groups linked to mesocarbons of the porphyrin ring, as shown in the inset of Figure 1. By substituting different metal ions at the central position or incorporating various organic compounds at peripheral positions, one is able to manipulate the spectroscopic characteristics of porphyrins to some extent. This is an interesting property because it allows the physical properties to be tuned to yield the optimum response for each different application.

To determine the influence of the central metal ion on the photophysical parameters of porphyrins, a systematic investigation with different ions is required. To partially fulfill this task, the present work investigates tetrapyridyl porphyrins with three different central metal ions: Zn^{2+} (ZnTPyP), Cu^{2+} (CuTPyP), Ni^{2+} (NiTPyP), which have valence states d^{10}, d^9, and d^8, respectively. We employed the Z-scan technique[7,8] with single pulses as well as with pulse trains[9] at 532 nm. Our results show that the closed-shell ZnTPyP behaves like the free base tetrapyridyl porphyrin,[10] while open-shell CuTPyP and NiTPyP present a completely different nonlinear absorption behavior. We also used other linear techniques such as UV−vis absorption spectroscopy and time-resolved fluorescence to obtain additional data to adjust our model.

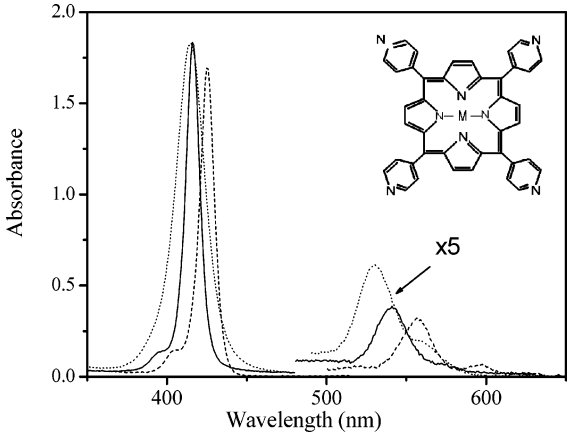

Figure 1. Absorbance spectrum (−log (I/I_0)) of NiTPyP (dotted line) CuTPyP (solid line) and ZnTPyP (dashed line). The inset shows the tetrapyridyl porphyrin structure, where M is the metal ion.

Experimental Section

Free base tetrapyridyl porphyrin (H_2TPyP) was obtained following the method described in ref 10. Metalloporphyrins were synthesized according to the general procedure: 0.250 g (4.04×10^{-4} mol) of H_2TPyP was dissolved in a mixture of 20

* Author to whom correspondence should be addressed. Fax: +55-16-3373-8085, ext 212. E-mail: newton@if.sc.usp.br.
† Instituto de Física de São Carlos, Universidade de São Paulo.
‡ Instituto de Química de São Carlos, Universidade de São Paulo.
§ Universidade Federal de São Carlos.

10.1021/jp052168i CCC: $30.25
Published on Web 08/17/2005

mL of acetic acid and 20 mL of dimethylformamide (DMF) under reflux. The corresponding metal salt was slowly added over a 1-h period, in a quantity of 2.5 times (in mol) that of H_2TPyP. The mixture was left under reflux for another 1 h, then the solution was cooled in an ice bath, and cold water was added to obtain a solid. The solid was filtered and washed with water to remove the excess of metal salt and dried in a vacuum. When necessary, the product was purified on an alumina column using a mixture of 95% chloroform and 5% methanol as eluent. The samples were dissolved in chloroform completed with 5% of methanol in volume and placed in a quartz cuvette (optical path: $L = 2$ mm) at room temperature for optical measurements.

UV−vis spectra were measured with a Cary-17 spectrophotometer, in samples that were prepared with a standard concentration of $N = 7 \times 10^{16}$ cm^{-3} (1.2×10^{-4} mol/L). After measuring the absorbance, the ground-state absorption cross-section, σ_0, was found through the relation $\sigma_0 = 2.3A/NL$, where A is the measured absorbance.

The fluorescence spectrum of ZnTPyP was determined with a portable spectrometer, using continuous wave excitation at 532 nm provided by the second harmonic of a diode-pumped Nd:YAG laser. The time-resolved fluorescence signal was acquired with a fast detector (rise time = 0.5 ns) plugged into a 1-GHz digital oscilloscope connected to a personal computer. In this case, the sample was pumped with a frequency-doubled Nd:YAG laser delivering single 70-ps pulses at 532 nm.

Nonlinear absorption measurements were carried out with the open-aperture Z-scan technique,[7,8] which essentially consists of measuring the sample transmittance as it translates through the focal plane of a tightly focused Gaussian beam. The pump source is a frequency-doubled, *Q*-switched and mode-locked Nd:YAG laser, delivering 70-ps pulses at 532 nm, in pulse trains containing about 20 pulses separated by 13.2 ns, operating with 10 Hz of repetition rate. A single pulse can be extracted from the *Q*-switch envelope with a Pockels cell, which favors the observation of fast electronic effects before the buildup of cumulative processes. Otherwise, the complete set of pulses under the *Q*-switch envelope can be used to discriminate between fast and accumulative nonlinearities in a technique named pulse-train Z-Scan (PTZ-scan).[9] The beam is focused to a diameter of 40 μm with an $f = 12$ cm lens. Several pulse trains (or single pulses) are acquired as the sample is scanned through the focus. Each peak of the pulse trains is proportional to the pulse fluence because the detection system has a response time longer than the 70-ps pulse duration. Normalizing each of these pulse trains to the one obtained when the sample is far from the focus produces a set of Z-scan signatures that can be used to map the absorptive nonlinearity along the *Q*-switch envelope and to determine fast (subnanosecond) and cumulative contributions. This is possible because the pulses in the train are separated by a time interval, which is longer than the lifetime of the first singlet excited state and, on the other hand, is much shorter than the lifetime of the first triplet state of ZnTPyP.[10−14] As we mentioned, a single 70-ps pulse can be used for the determination of fast electronic nonlinearities, but since metalloporphyrins may possess very fast relaxation rates, we also carried out Z-scan experiments with 120-fs pulses at 532 nm to make sure that triplet states are not populated. These pulses were provided by an optical parametric amplifier (OPA) pumped by 150-fs pulses at 775 nm coming from a 1-kHz Ti:sapphire chirped pulse amplified system.

Results and Discussion

Absorption and Fluorescence Measurements. The absorption spectra shown in Figure 1 present the characteristics bands of porphyrins complexes.[6] The B (Soret)-bands are located around 430, 416, and 415 nm for ZnTPyP, CuTPyP, and NiTPyP, respectively, while the Q-bands cover the region from 500 to 650 nm. Therefore, the 532 nm used in the experiments excites just Q-bands, and at this wavelength the ground-state absorption cross-sections were found to be $\sim 2.1 \times 10^{-17}$ cm^2 for ZnTPyP, $\sim 5.3 \times 10^{-17}$ cm^2 for CuTPyP, and $\sim 5.5 \times 10^{-17}$ cm^2 for NiTPyP.

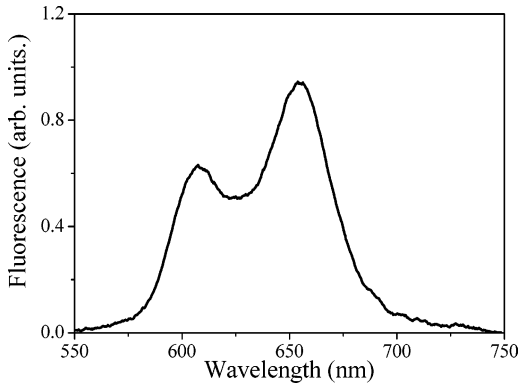

Figure 2. Fluorescence spectrum of ZnTPyP with excitation at 532 nm.

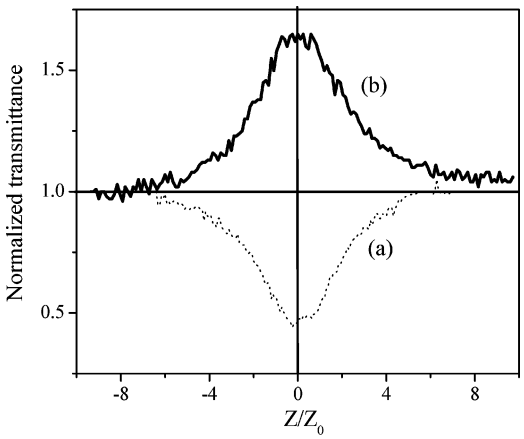

Figure 3. Typical Z-scan signature for (a) ZnTPyP and (b) CuTPyP, obtained with single 70-ps pulses at an intensity of 4 GW/cm^2, at the focus. The concentrations used are respectively: 3 and 2.4×10^{-4} mol/L.

Figure 2 presents the ZnTPyP fluorescence spectrum, where the two strongest peaks observed at 607 and 655 nm are, respectively, related to the absorption bands Q(0,0) and Q(0,1).[15] The fluorescence decay curve, not shown here, was successfully adjusted with a monoexponential function, yielding a fluorescence lifetime of 1.6 ns, which is in agreement with the results reported in ref 16. No fluorescence signal is observed in CuTPyP and NiTPyP samples. As reported in the literature, there is indeed a dissimilar spectroscopic behavior between ZnTPyP, which is a closed-shell metal porphyrin, and open-shell metal porphyrins such as CuTPyP and NiTPyP.[6,16] As we will discuss later, a difference is also observed in the nonlinear optical properties.

ZnTPyP Excited-State Dynamics. The Z-scan signature obtained at 532 nm with single 70 ps-duration pulses clearly shows a reverse saturable absorption (RSA) process in ZnTPyP, as depicted in Figure 3a. Since the intersystem crossing time (τ_{isc}) of closed-shell porphyrins is in the nanosecond time scale,[10,17] the triplet state population can be neglected, and the singlet excited-state cross-section is determined by observing

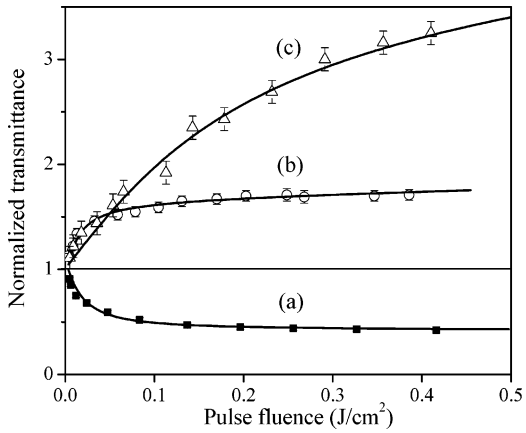

Figure 4. Normalized transmittance versus 70-ps pulse fluence for (a) ZnTPyP, (b) CuTPyP, and (c) NiTPyP. The concentrations used are, respectively, 3, 2.4, and 4.6×10^{-4} mol/L. The solid lines are the fittings obtained with the respective models.

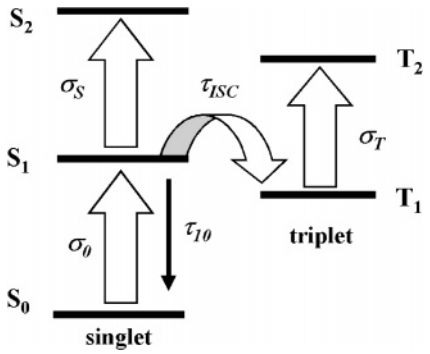

Figure 5. Five-energy-level diagram used to find the excited-state dynamics of ZnTPyP.

the saturation behavior occurring in single-pulse Z-scan measurements as a function of the pulse fluence, as shown in Figure 4a.

To obtain the singlet excited-state cross-section from the saturation behavior, we have to take into account that the measurements are carried out in the absorptive region, and in that case they present a nonlinear response that is due to a sequential two-photon absorption. Therefore, we use a generalized phenomenological model consisting of three singlet states (the ground S_0, the first excited S_1, and the second excited S_2) and two triplet states (the first excited T_1 and the second excited T_2), as shown in Figure 5. The absorption from the ground state excites the Q-band of the porphyrin molecule, and because Zn^{2+} is a closed-shell ion, a very small influence of *d* levels of the ion on $\pi-\pi^*$ transitions of the ligand is expected. Consequently, just $\pi-\pi^*$ transitions are predominant on the excited-state dynamics.[18]

An intense laser pulse redistributes the population of molecules between the ground and excited states, causing a transient modification in the optical properties of the material. According to the five-energy-level diagram, molecules excited to the first excited-singlet-level S_1 as a result of a one-photon absorption can either decay back to the ground singlet state S_0 or undergo an intersystem crossing to the triplet state T_1, which is assumed to be long-lived. However, since the pulse duration (70 ps) is much shorter than the intersystem crossing time (~ns), the five-energy-level model for the single-pulse experiments reduces to a three-level diagram, because the intersystem crossing from $S_1 \rightarrow T_1$ is negligible, and we can assume a vanishing triplet population. The populations of higher excited singlet levels are neglected because they are too short-lived. Moreover, stimulated emission can also be neglected because of the extremely fast relaxation to lower energy vibrational levels that are not in resonance with the incident photon. In this case, the nonlinear absorption effect is due only to the difference between the cross-sections of ground and excited singlet states.

The expression giving the fluence reaching the detector was derived previously as[10,19]

$$\frac{dF}{dz'} = -\alpha_0\left\{F + \left(\frac{\sigma_S}{\sigma_0} - 1\right)\left(F + \frac{h\nu}{\sigma_0}\left[\exp\left\{-\frac{\sigma_0 F}{h\nu}\right\} - 1\right]\right)\right\} \quad (1)$$

where

$$F(t) = \int_{-\infty}^{t} I(t)\, dt$$

is the fluence from $-\infty$ to t, and I is the irradiance. We note that for $\sigma_s > \sigma_g$ a reverse saturable absorption process occurs, while for $\sigma_s < \sigma_g$ saturable absorption takes place. Also, the lower is the ground-state absorption cross-section, the higher is the possibility of obtaining good reverse saturable absorption signals.

To find the energy reaching the detector after a single laser pulse, we numerically integrate this equation over the sample thickness and over the beam cross-section, assuming it to present a Gaussian transverse profile. The result is normalized to the linearly transmitted energy, $\epsilon = \epsilon_0 \exp\{-\alpha_0 L\}$. The fluence dependence of the normalized transmittance is used to fit the data in Figure 4a, providing the value of 4.9×10^{-17} cm^2 for the excited singlet cross-section σ_S. Z-scan measurements carried out with 120-fs pulses at 532 nm results in the same value for the singlet excited-state absorption. This is expected because, for both picosecond and femtosecond pulses, only the excited singlet state is responsible for the RSA.

In measurements carried out with pulse trains, the triplet state contributes to the optical nonlinearity because the duration of the *Q*-switch envelope (≈200 ns) is long enough to accumulate population in it. Therefore, each pulse of the train perceives a fast nonlinear absorption associated with transitions occurring in the singlet manifold, accompanied by a slower contribution from the triplet manifold, which depends on the T_1 state population accumulated from previous pulses of the train. By neglecting the triplet relaxation, the five-energy-level model leads to following set of differential equations for the population fractions at each level:

$$\frac{dn_{S0}}{dt} = -W_{S0\rightarrow S1} n_{S0} + \frac{n_{S1}}{\tau_{10}} \quad (2a)$$

$$\frac{dn_{S1}}{dt} = W_{S0\rightarrow S1} n_{S0} - \left(\frac{1}{\tau_{10}} + \frac{1}{\tau_{isc}}\right) n_{S1} \quad (2b)$$

$$\frac{dn_{T1}}{dt} = \frac{n_{S1}}{\tau_{isc}} \quad (2c)$$

where

$$W_{S0\rightarrow S1} = \frac{\sigma_0 I}{h\nu}$$

is the upward one-photon transition rate, n_{S0}, n_{S1}, and n_{T1} are, respectively, the population fractions of levels S_0, S_1, and T_1, with $n_{S0} + n_{S1} + n_{T1} = 1$ being the normalization condition. τ_{isc} is the intersystem crossing time, and $1/\tau_{10}$ is the population decay rate from the S_1 to the S_0 state, which considers both

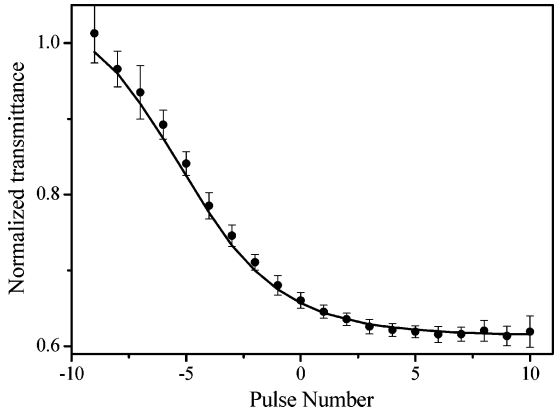

Figure 6. Pulse-train measurements in ZnTPyP, where the strongest pulse of the train was labeled "0". The solid line is the best fitting obtained with the five-energy-level diagram.

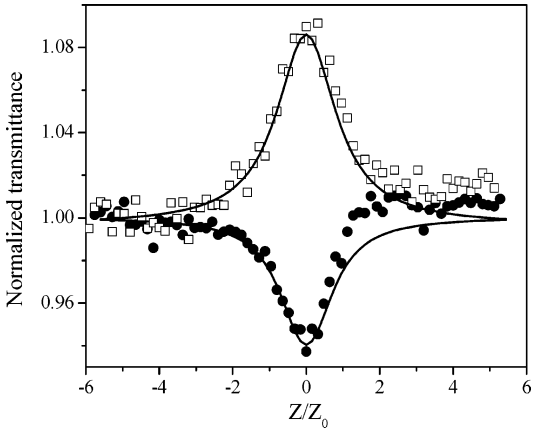

Figure 7. Z-scan measurements at the femtosecond scale for CuTPyP (full circles) and NiTPyP (open squares). The solid lines are fittings obtained with the singlet manifold.

radiative and internal conversion decay paths. The fluorescence lifetime τ_f can be related to τ_{isc} and τ_{10} according to $1/\tau_f = 1/\tau_{10} + 1/\tau_{isc}$. Since the photophysical parameters related to the singlet manifold are already known, we can now determine the triplet cross-section, σ_T, and the intersystem crossing time, τ_{isc}. To do so, the above rate equations were solved numerically using the temporal intensity pattern of the *Q*-switched/mode-locked pulse train actually employed in our Z-scan experiments and the initial conditions $n_{S0}(-\infty) = 1$, $n_{S1}(-\infty) = n_{T1}(-\infty) = 0$, producing new values for the populations at each pulse. This procedure yields the population dynamics necessary to determine the excited-state parameters. The transmittance evolution is found according to

$$\frac{dI}{dz} = -N[n_{S0}\sigma_0 + n_{S1}\sigma_S + n_{T1}\sigma_T] \qquad (3)$$

Numerically solving eqs 2 and 3 using σ_0, τ_f, and σ_S obtained from previous measurements and normalizing the result to the linearly transmitted energy, the values of the intersystem crossing time and triplet excited-state absorption cross-section are obtained from the best fitting of the pulse-train Z-scan data, as depicted in Figure 6. The values obtained are 3.8×10^{-17} cm^2 and 6 ns for σ_T and τ_{isc}, respectively. We used a maximum concentration of 2.4×10^{-4} mol/L in these experiments because higher values could produce the formation of molecular aggregates.

CuTPyP Excited-State Dynamics. CuTPyP molecules present a nonlinear absorption behavior strongly dependent on the pulse duration used, indicating a different excited-state dynamics from that of ZnTPyP. Such behavior is attributed to different relative populations of the excited singlet and triplet levels. For 120-fs pulses, CuTPyP presents the RSA process shown as solid circles in Figure 7. Since the pulse duration is too short compared to the intersystem crossing time, just singlet levels contribute to the nonlinear absorption signal. Therefore, the same model used to analyze the optical nonlinearity of ZnTPyP subjected to 70-ps pulses, where just the singlet manifold is considered, can be applied in this case. The only adjustable parameter is the excited singlet absorption cross-section and the value found for it after fitting the Z-scan curve is 5.7×10^{-17} cm^2.

On the other hand, a saturable absorption (SA) process is observed for 70-ps pulses, as already depicted in Figure 3. This fact suggests that differently from 120-fs pulses, the intersystem crossing rate is high enough to allow the triplet state to be populated. Is known that the intersystem crossing time of copper porphyrins varies from hundreds of femtoseconds to tens of picoseconds.[20,21] In particular, due to the coupling of the unpaired electron in the *d* level of Cu^{+2} and π orbitals of the porphyrin ring, a tripdoublet $^2T_1(\pi,\pi^*)$ and a quartet $^4T_1(\pi,\pi^*)$ are formed. However, as the energy difference between these two levels is small in comparison with the photon energy used,[20] we can consider these two levels as just a single excited triplet level and use again the complete five-energy-level diagram. Moreover, copper porphyrins have a charge transfer level next to the triplet state which together with d−d states decreases considerably its phosphorescence lifetime and intersystem crossing time.[20,22]

To investigate the nonlinear absorption dynamics for single 70-ps pulses, we performed a set of Z-scan measurements as a function of the pulse fluence. The result shown in Figure 4b can be explained assuming that the intersystem crossing time has a much higher quantum yield than that of the $S_1 \rightarrow S_0$ relaxation. Therefore, the rate $1/\tau_{10}$ can be set to zero in eq 2, and the simpler resulting set of rate equations is solved by considering the single 70-ps pulse with a temporal Gaussian profile. This procedure yields the population in each level, and the time evolution of the absorption coefficient is calculated with eq 3, where the intersystem crossing time and the triplet absorption cross-section are the fitting parameters. The values obtained were 3.7×10^{-17} cm^2 for σ_T and ~10 ps for τ_{isc}. No accumulative effect was observed in PTZ-scan measurements, which indicates that the phosphorescence lifetime is less than 13.2 ns. This value has the same order of magnitude as those found in the literature for copper porphyrins.

NiTPyP Excited-State Dynamics. Differently from the copper ion, Ni^{2+} has just eight electrons distributed in the *d* orbital, six of them filling d_{xy}, d_{xz}, and d_{yz} orbitals. In noncoordinating solvents (as is the case of the chloroform solvent used), the remaining two electrons reside in the d_z^2 orbital with a paired configuration, resulting in a diamagnetic porphyrin molecule where the singlet ground-state S_0 is the $^1A_{1g}$ state.[23] The energy-level diagram appropriate to describe the excited-state dynamics of NiTPyP is shown in Figure 8. Upon excitation to the Q-band, the molecule is promoted to an excited singlet level $^1Q(\pi,\pi^*)$ and rapidly relaxes to level $^1B_{1g}(d_{z^2},d_{x^2-y^2})$ in a few picoseconds or even less.[24] Owing to this ultrafast relaxation, these two levels can be considered as just one singlet level. Another possible path for molecules relaxing from the $^1Q(\pi,\pi^*)$ level would be through a $\pi-\pi^*$ intersystem crossing transition to level $^3T_2(\pi,\pi^*)$, later on suffering a triplet−triplet charge-transfer transition to $^3B_{1g}(d_{z^2},d_{x^2-y^2})$, via $^3T_1(\pi,\pi^*)$. However, we believe that this path can be neglected because

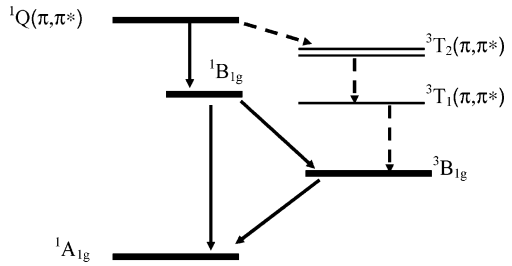

Figure 8. Energy-level diagram for NiTPyP.

transitions between pure $\pi-\pi^*$ orbitals occur in a time scale of a few nanoseconds.[6] Thus our experimental data can be well explained by an energy-level diagram similar to that shown in Figure 5, with the levels ^1Q and $^1B_{1g}$ represented by the level S_1.

According to the literature, a molecule in the singlet level $^1B_{1g}$ can suffer an intersystem crossing to the triplet level $^3B_{1g}$, corresponding to level T_1 in Figure 5, in less than 15 ps.[24] From T_1, the molecule relaxes to the ground state with a time that ranges from 250 to 300 ps.[25] Another possible decay for the molecule in level S_1 is through the relaxation $S_1 \rightarrow S_0$. Nevertheless, to our knowledge, and differently from $S_1 \rightarrow T_1$ and $T_1 \rightarrow S_0$, this transition was never measured in picosecond excited-state absorption experiments. This fact can be explained by considering that the transition is too fast to be detected by the resolution of the experiments performed up to now. As the experiments reported in the literature have a time resolution of tens of picoseconds, they will not detect this relaxation if it occurs in a time of a few picoseconds or less. The assumption that this decay time is so fast is supported by the fact that in Ni porphyrins, an open d shell affects the singlet decay rate, reducing its lifetime. To verify this behavior, we have performed Z-scan measurements with both 120-fs and 70-ps pulses. Assuming that the intersystem crossing is around a few picoseconds, we fitted the Z-scan measurements with 120-fs pulses as done for CuTPyP, where the unique fitting parameter considered is σ_S. The result is shown in Figure 7, and the best fit was achieved with $\sigma_S = 4.9 \times 10^{-17}$ cm^2.

Results with 70-ps single pulses were adjusted considering again the five-level-energy diagram as done for CuTPyP, with the difference that a 1-ps singlet lifetime was taken into account. This last assumption is supported by the fact that it is necessary to explain the higher saturation intensity of the nonlinear process observed for NiTPyP in comparison with CuTPyP. Thus, the rate equations that describe the population dynamics for NiTPyP at a picosecond scale are the same as in eq 2. This set of equations was solved, and the time evolution of the absorption coefficient was calculated again with eq 3. The intersystem crossing time and the triplet absorption cross-section are the fitting parameters considered. The 70-ps measurement is shown in Figure 4c, and the values obtained for the best fitting are 3.0×10^{-17} cm^2 for σ_T, $\sim$10 ps for τ_{isc}, and 1 ps for the singlet decay time. As for CuTPyP, no accumulative effect was observed in PTZ-scan measurements. This fact was expected because the phosphorescence lifetime for Ni porphyrins is around 250 ps.

Conclusions

In summary, we have measured the excited-state absorption for three tetrapyridyl metalloporphyrins (Zn^{2+}, Cu^{2+}, and Ni^{2+}) using the Z-scan technique. The behavior of ZnTPyP was found to be different from that of the open-shell CuTPyP and NiTPyP. It presents a reverse saturable absorption process at time scales ranging from femtosecond to nanosecond, and whose time evolution could be easily described with a five-energy-level diagram. The subnanosecond process is attributed to the excited-singlet-state population, while the accumulative nanosecond process is related to the triplet-state absorption. On the other hand, CuTPyP and NiTPyP do not exhibit an accumulative absorption process at the nanosecond scale. At the picosecond temporal scale, they exhibit saturable absorption processes; at the femtosecond scale, a reverse saturable absorption is observed in CuTPyP, and a saturable process is found in NiTPyP. These processes are related to the excited singlet state at the femtosecond scale and to the triplet state absorption at the picosecond time scale. The absence of cumulative nonlinear processes at the nanosecond scale is attributed to fast relaxation times occurring in the excited states. This behavior can be satisfactorily explained by considering the influence of the open *d* level of the central ion on the deactivation routes of porphyrins. A marked difference is observed in the intensity of saturation of the nonlinear absorption process for the open-shell porphyrins. This fact is well explained assuming that the $^1B_{1g}$ level acts on the first excited singlet level of NiTPyP, reducing the lifetime of the system.

The procedure adopted in this work allowed us to discriminate among contributions from different excited states in the nonlinear absorption process. By fitting Z-scan data, we were able to determine the excited-state spectroscopic parameters as well as the characteristic relaxation times.

Acknowledgment. We gratefully acknowledge the support of Fundação de Amparo à Pesquisa do Estado de São Paulo (FAPESP) and Conselho Nacional de Desenvolvimento Científico e Tecnológico (CNPq).

References and Notes

(1) Loppacher, C.; Guggisberg, M.; Pfeiffer, O.; Meyer, E.; Bammerlin, M.; Luthi, R.; Schlittler, R.; Gimzewski, J. K.; Tang, H.; Joachim, C. *Phys. Rev. Lett.* **2003**, *90*, 066107−1.

(2) Su, W. J.; Cooper, T. M.; Brant, M. C. *Chem. Mater.* **1998**, *10*, 1212.

(3) Blau, W.; Byrne, H.; Dennis, W. M.; Kelly, J. M. *Opt. Commun.* **1985**, *56*, 25.

(4) Voet, D.; Voet, J. G. *Biochemistry*; John Wiley & Sons Inc.: New York, 1995.

(5) Fisher, A. M. R.; Murphree, A. L.; Gomer, C. J. *Lasers Surg. Med.* **1995**, *17*, 2.

(6) Kalyanasundaram, K. *Photochemistry of polypyridine and porphyrin complexes*; Academic Press: San Diego, 1992.

(7) Sheik-Bahae, M.; Said, A. A.; Van Stryland, E. W. *Opt. Lett.* **1989**, *14*, 955.

(8) Sheik-Bahae, M.; Said, A. A.; Wei, T.; Hagan, D. J.; Van Stryland, E. W. *IEEE J. Quantum Electron.* **1990**, *26*, 760.

(9) Misoguti, L.; Mendonça, C. R.; Zilio, S. C. *Appl. Phys. Lett.* **1999**, *74*, 1531.

(10) Barbosa Neto, N. M.; De Boni, L.; Rodrigues, J. J.; Misoguti, L.; Mendonça, C. R.; Dinelli, L. R.; Batista, A. A.; Zilio, S. C. *J. Porphyr. Phthalocya.* **2003**, *7*, 452.

(11) Mendonça, C. R.; Gaffo, L.; Moreira, W. C.; Oliveira, O. N., Jr.; Zílio, S. C. *Chem. Phys. Lett.* **2000**, *323*, 300.

(12) Corrêa, D. S.; De Boni, L.; Santos, D. S., Jr.; Barbosa Neto, N. M.; Oliveira, O. N., Jr.; Misoguti, L.; Zílio, S. C.; Mendonça, C. R. *Appl. Phys. B* **2002**, *74*, 559.

(13) Mendonça, C. R.; Barbosa Neto, N. M.; Batista, P. S.; Souza, M. F.; Zílio, S. C. *Chem. Phys. Lett.* **2002**, *361*, 383.

(14) Gonçalves, P. J.; De Boni, L.; Barbosa Neto, N. M.; Rodrigues, J. J., Jr.; Zílio, S. C.; Borissevitch, I. E. *Chem. Phys. Lett.* **2005**, *407*, 236.

(15) Qian, D.-J.; Planner, A.; Miyake, J.; Frackowiak, D. *J. Photochem. Photobiol., A* **2001**, *144*, 91.

(16) Kobayashi, T.; Straub, K. D.; Rentzepis, P. M. *Photochem. Photobiol.* **1979**, *29*, 925.

(17) Kalyanasundaram, K. *Inorg. Chem.* **1984**, *23*, 2453.

(18) Donzello, M. P.; Dini, D.; D'Arcangelo, G.; Ercolani, C.; Zhan, R.; Ou, Z.; Stuzhin, P. A.; Kadish, K. M. *J. Am. Chem. Soc.* **2003**, *125*, 14190.

(19) Wei, T. H.; Huang, T. H.; Wen, T. C. *Chem. Phys. Lett.* **1999**, *314*, 403.
(20) Sazanovich, I. V.; Ganzha, V. A.; Dzhagarov, B. M.; Chirvony, V. S. *Chem. Phys. Lett.* **2003**, *382*, 57.
(21) Kobayashi, T.; Huppert, D.; Straub, K. D.; Rentzepis, P. M. *J. Chem. Phys.* **1979**, *70*, 1720.
(22) Yan, X. W.; Holten, D. *J. Phys. Chem.* **1988**, *92*, 5982.
(23) Kim, D.; Holten, D. *Chem. Phys. Lett.* **1983**, *98*, 584.
(24) Kim, D.; Kirmaier, C.; Holten, D. *Chem. Phys.* **1983**, *75*, 305.
(25) Chirvonyi, V. S.; Dzhagarov, B. M.; Timinskii, Y. V.; Gurinovich, G. P. *Chem. Phys. Lett.* **1980**, *70*, 79.